Electronic Supplementary Information

In-situ formed CuSn alloy from multivariate metal-organic frameworks for tunable CO_2 electroreduction

Xuheng Li,[1,+] Chen Qin,[1,+] Chunli Wang,[2] Fuping Pan[1,3,*] and Kai-Jie Chen[1,*]

[1] School of Chemistry and Chemical Engineering, Northwestern Polytechnical University, Xi'an, Shaanxi 710072, China.

[2] Research Center for Environmental Material and Pollution Control Technology, National Engineering Laboratory for VOCs Pollution Control Material & Technology, University of Chinese Academy of Sciences, Beijing, 101408, P. R. China.

[3] Chongqing Innovation Center, Northwestern Polytechnical University, Chongqing, 401135, China.

[+] These authors contributed equally to this work.

[*] E-mails: fupingpan@nwpu.edu.cn; ckjiscon@nwpu.edu.cn.

Experimental section

Chemicals

N, N-dimethylformamide (DMF, 99%), Triethylamine (TEA, 99%), ethanol (98%), benzene dicarboxylic acid (H_2BDC, 99%), $CuCl_2$ (98%), $SnCl_2$ (98%), and isopropanol (IPA, 99%) were purchased from Sinopharm Chemical Reagent Co., Ltd (Shanghai, China) with analytical grade. Potassium hydrogen carbonate ($KHCO_3$, AR) was purchased from Sinopharm Chemical Reagent Co., Ltd (Shanghai, China). Nafion (5 wt%) was purchased from Shanghai Macklin Biochemical Co., Ltd. Dimethyl sulfoxide and deuterium water were purchased from Shanghai Yien Chemical Technology Co., Ltd. All chemicals were used as received without further purification.

Catalysts Preparation

Synthesis of CuBDC: Cu-MOF nanosheet was prepared by a facile method. Firstly, 34 mL DMF, 10 mL ethanol, and 10 mL water were mixed in a 100 mL polytetrafluoroethylene (PTFE) tube. Next, 1.5 mmol H_2BDC was dissolved into the mixed solution under ultrasonication. Subsequently, 1.5 mmol $CuCl_2$ was added. Until $CuCl_2$ was dissolved, 1.6 mL TEA was quickly injected into the solution. A uniform colloidal suspension was obtained by stirring the above solution for 5 min. Afterward, the colloidal solution was continuously ultrasonicated for 8 h (40 kHz) under airtight conditions. The resulting blue precipitate was rinsed with DMF and ethanol (5 times). Finally, the produced sample was centrifuged and followed by drying in air.

Synthesis of CuSnBDC: The procedure is similar to the synthesis of CuBDC. $CuCl_2$, and $SnCl_2$ (Cu: Sn=1: 1, 2: 1, 4: 1, 9: 1, 19: 1, respectively) were added to a mixed solution of DMF, Ethanol, and H_2O, in which H_2BDC was dissolved. The subsequent steps were the same as the treatment of Cu-BDC.

Catalysts Characterization

The morphology, structure, and composition of catalysts were characterized by scanning electron microscopy (SEM, FEI Verios G4), transmission electron microscopy (TEM, FEI Talos F200X), high-angle annular dark-field scanning transmission electron microscopy (HAADF-STEM, FEI Themis Z), X-ray diffraction (XRD, MiniFlex), X-ray photoelectron spectroscopy (XPS, Kratos AXIS Ultra DLD), FT-IR spectra (Thermo Scientific Nicolet iS 50 FTIR), and inductively coupled plasma optical emission spectrometer (ICP-OES, NexIONTM 350D). N_2 sorption isotherms were measured at 77 K on a Quantachrome Instrument ASiQMVH002–5 after 12 h pretreatment. The pore size distributions were fitted by non-local density functional theory (NLDFT). Raman spectra were recorded using a Raman spectrometer (WITec Alpha 300R).

Electrochemical Measurements

All electrochemical measurements were conducted on an electrochemical workstation (Gamry Interface 1000E). To prepare the cathode electrode in the H cell, a mixture that contains 3 mg of catalysts, 200μL of water, 370 μL of isopropanol, and 30 μL of Nafion ionomer solution (5 wt% in isopropanol) was first sonicated for 120 min to obtain a catalyst ink. Then, 200 μL of the catalyst ink was drop-casting onto a gas diffusion layer (GDL) five times to achieve a catalyst loading of ~1.0 mg cm^{-2}. The alloy catalysts in the H cell were obtained at a constant current density of −20 mA cm^{-2} for 60 min in a standard three-electrode H cell system supplied with CO_2 gas. The electrochemical H cell includes a gas chamber, a cathodic chamber, and an anodic chamber. A 0.1 M $KHCO_3$ solution was used as the anolyte and catholyte, and the ionic exchange membrane separated the cathode chamber and an anode chamber (Fumasep PK 130, Fuel Cell Stores). A piece of Pt was used as the counter electrode, and a saturated Ag/AgCl was used as the reference electrode. To prepare the electrode in a flow cell, a mixture that contains 5 mg of catalysts, 2 mL of isopropanol, and 50 μL of Nafion ionomer solution (5 wt% in isopropanol) was first sonicated for 120 min to obtain a catalyst ink. Then, 2 mL of the catalyst ink was sprayed onto a gas diffusion layer to achieve a catalyst loading of ~1.0 mg cm^{-2}. The alloy catalysts were obtained at a constant current density of −300 mA cm^{-2} for 30 min in a standard three-electrode flow cell system supplied with CO_2 gas. The electrochemical flow cell includes a gas chamber, a cathodic chamber, and an anodic chamber. A 1.0 M $KHCO_3$ solution was used as the anolyte and catholyte, and the ionic exchange membrane separated the cathode chamber and anode chamber (Fumasep PK 130, Fuel Cell Stores). A piece of nickel foam was used as the counter electrode, and a saturated Ag/AgCl was used as the reference electrode. The high-purity CO_2 (99.999%) was introduced on the back side of the gas diffusion layer, and the electrolyte flowed in both cathodic and anodic chambers with a flow rate of 2 mL min^{-1}. The following devices for the evaluation of CO_2RR performance are the same as the preparation of cathodes. The electrochemical active surface area (ECSA) were determined by measuring double-layer capacitance (C_{dl}). C_{dl} was determined by measuring the capacitive current associated with double-layer charging from the scan-rate dependence of cyclic voltammogram (CV). All potentials were converted to the reversible hydrogen electrode by E (RHE) = E (Ag/AgCl) + 0.197 V + 0.0591 V × pH without iR compensation.

Product Analysis

The gaseous products were monitored by an online gas chromatograph (GC, GC9790PLUS) equipped with a thermal conductivity detector (TCD) and a flame ionization detector (FID). The liquid products in cathode chambers were collected after electrolysis and analyzed by ^{1}H nuclear magnetic resonance (NMR, Bruker AV400) using DMSO as the internal standard and D_2O as a proton signal source.

The Faraday efficiency (FE) of gas products was calculated by the following equation:

$$FE\% = \frac{I}{I_{total}} = \frac{zFnV}{I_{total}} \times 100$$

Where I is the partial current density of a specific product. I_{total} is the total current density collected in the bulk electrolysis at an applied potential. z is the number of electrons involved in the formation of a specific product. F is the Faraday constant, 96485 C mol^{-1}. n is the mole fraction of the product. V is the gas volumetric flow rate of gas.

The FE of the liquid products was calculated as:

$$FE = z \cdot F \cdot \frac{n}{Q}$$

Where z is the number of electrons transferred per mole of gas product, F is Faraday constant (96500 C mol^{-1}), n is the total amount of the liquid products determined from NMR (mole), Q is the total amount of charge passed through the cathode (A·s).

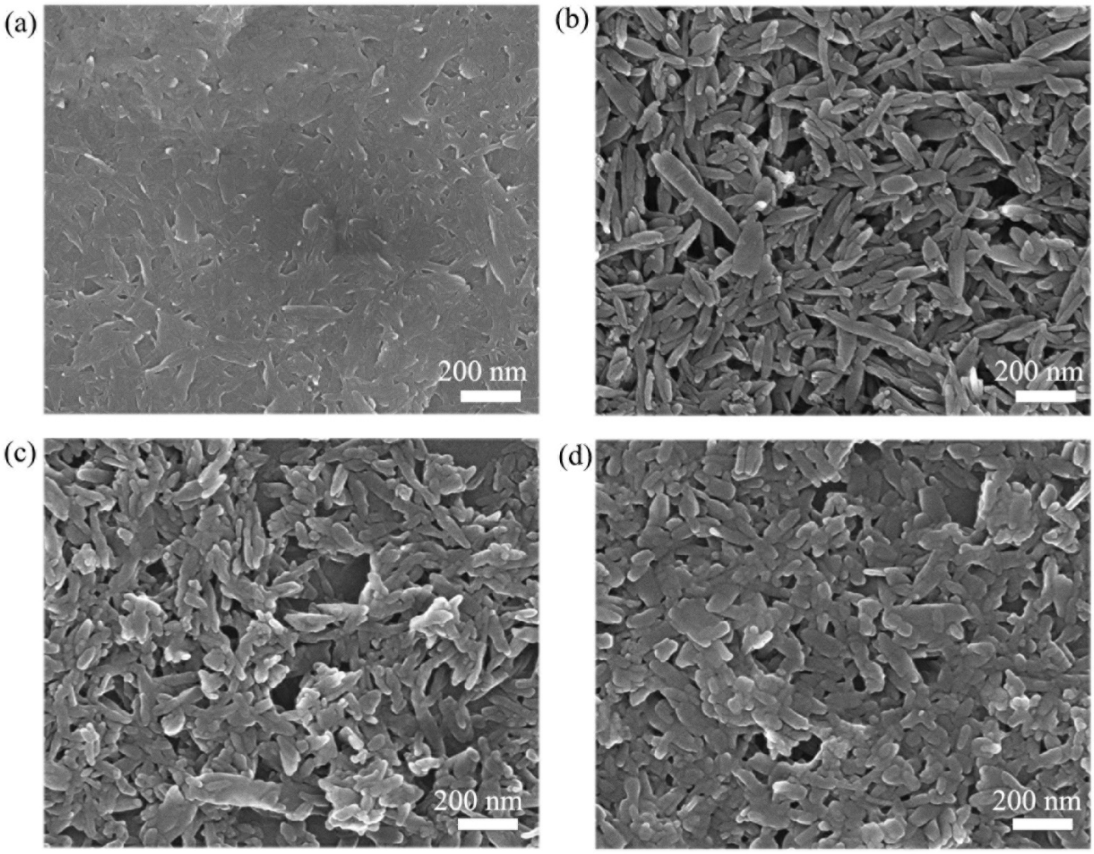

Fig. S1 SEM images of (a) CuBDC, (b) CuSnBDC (2: 1), (c) CuSnBDC (9: 1), and (d) CuSnBDC (19: 1).

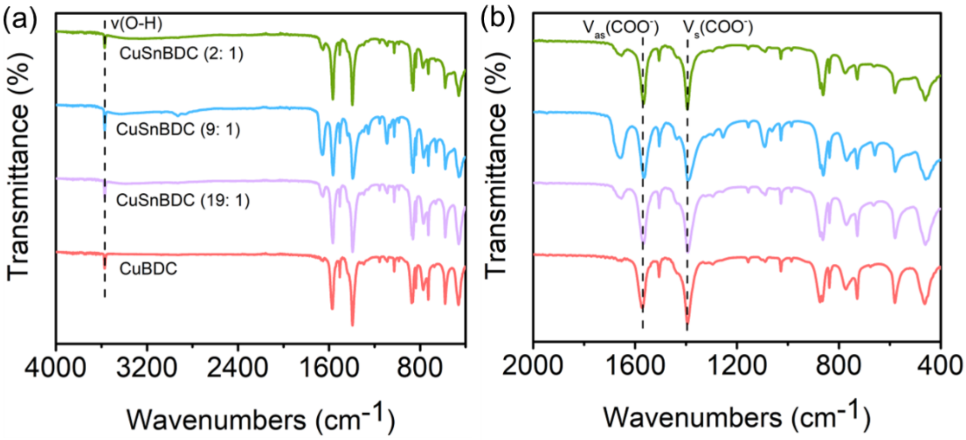

Fig. S2 FT-IR spectra of CuBDC and CuSnBDC.

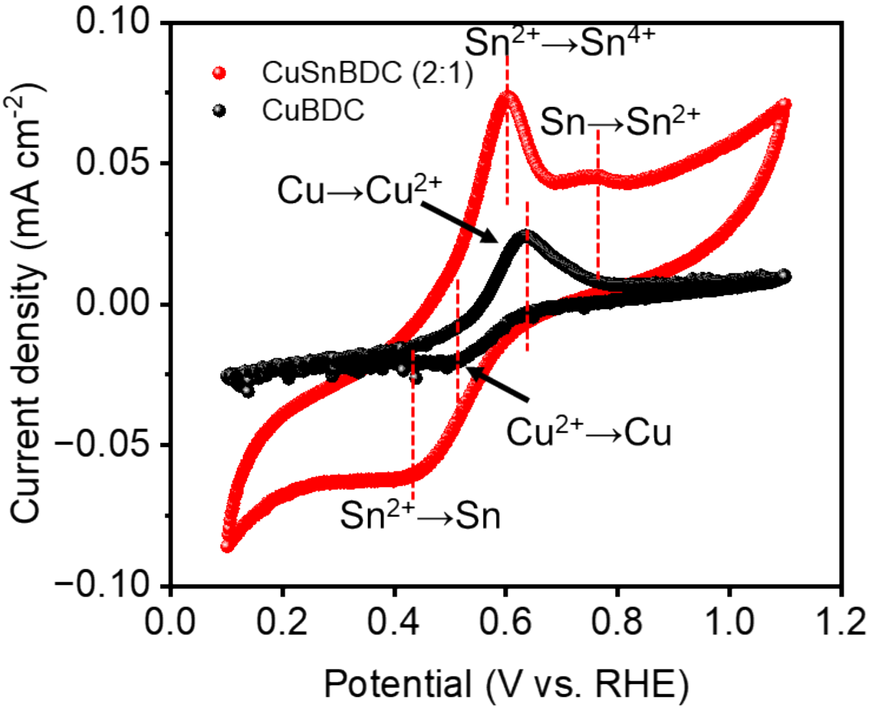

Fig. S3 Cyclic voltammogram curves of CuSnBDC and CuBDC loaded on the carbon paper.

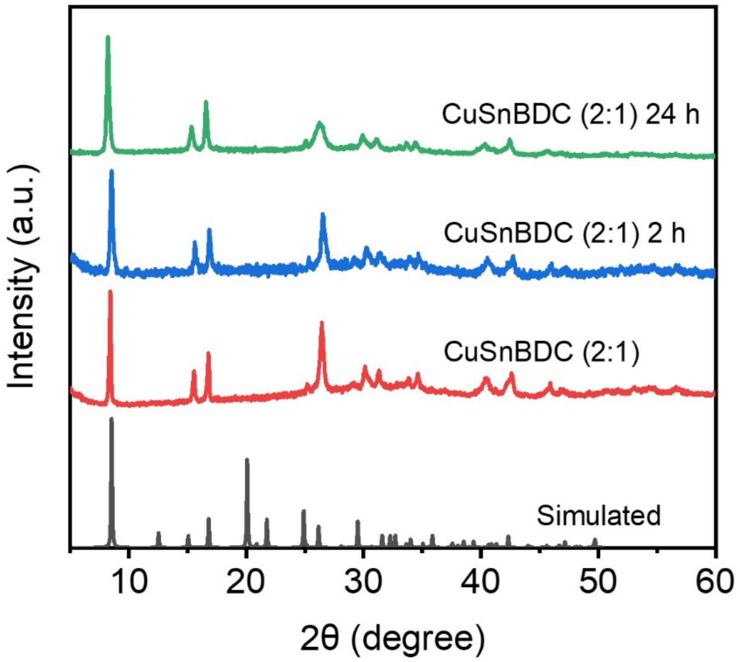

Fig. S4 XRD patterns of CuSnBDC after soaking in 0.1 M $KHCO_3$ for 2 h and 24 h.

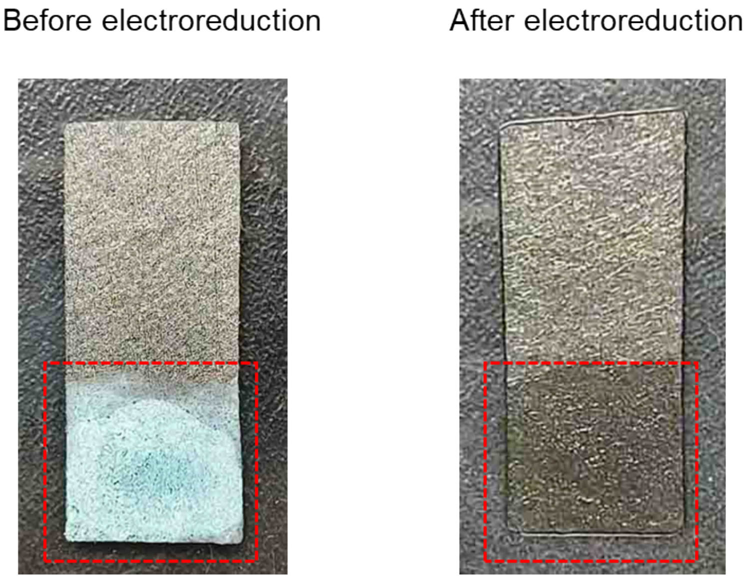

Fig. S5 Optical images of CuSnBDC loaded on the carbon paper before and after reduction.

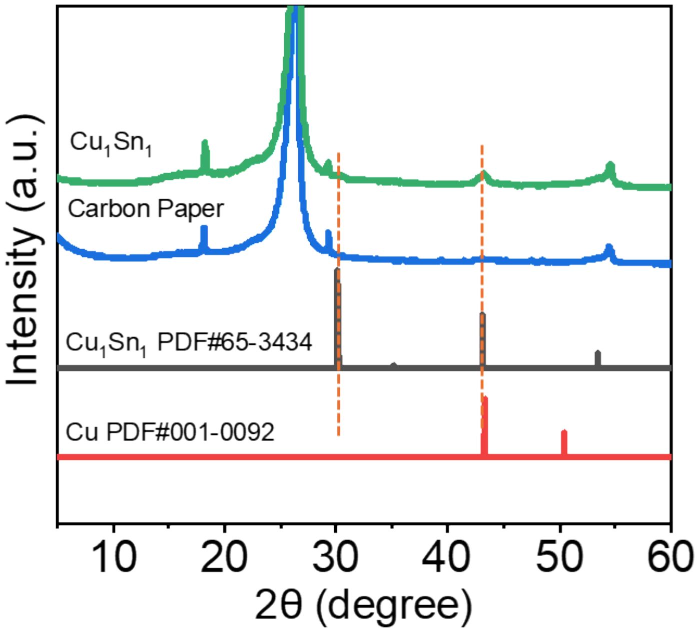

Fig. S6 XRD pattern of Cu_1Sn_1 alloy.

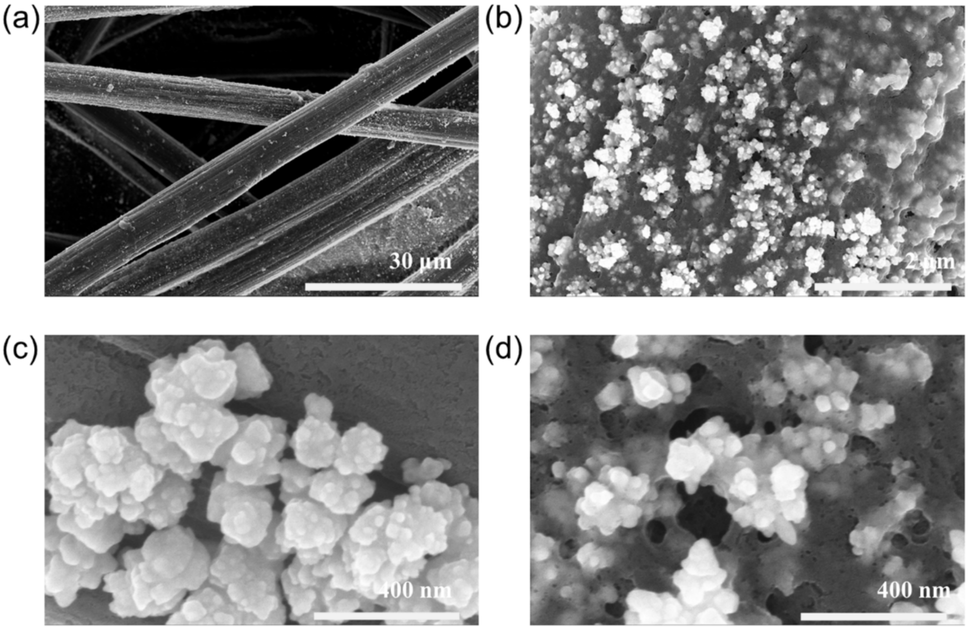

Fig. S7 (a)-(d) SEM images of the Cu_2Sn_1 alloy catalyst on carbon fiber.

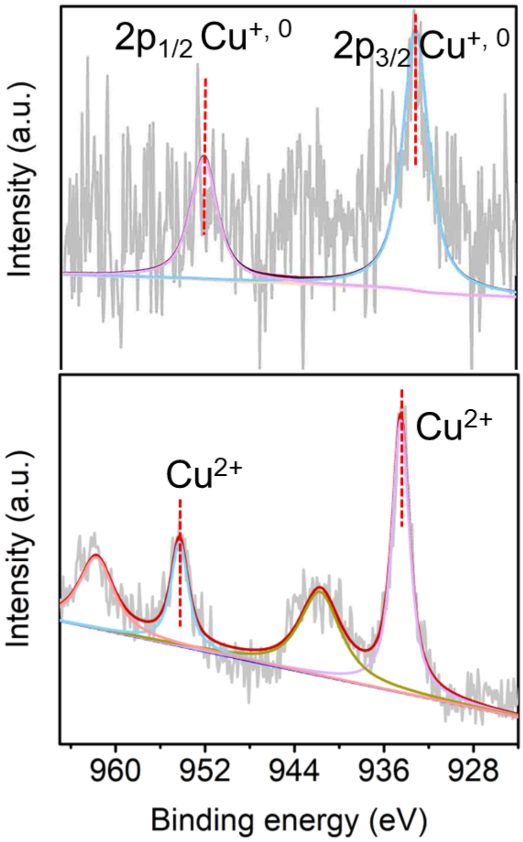

Fig. S8 Cu 2p for Cu catalyst (the upper) and CuBDC (the lower).

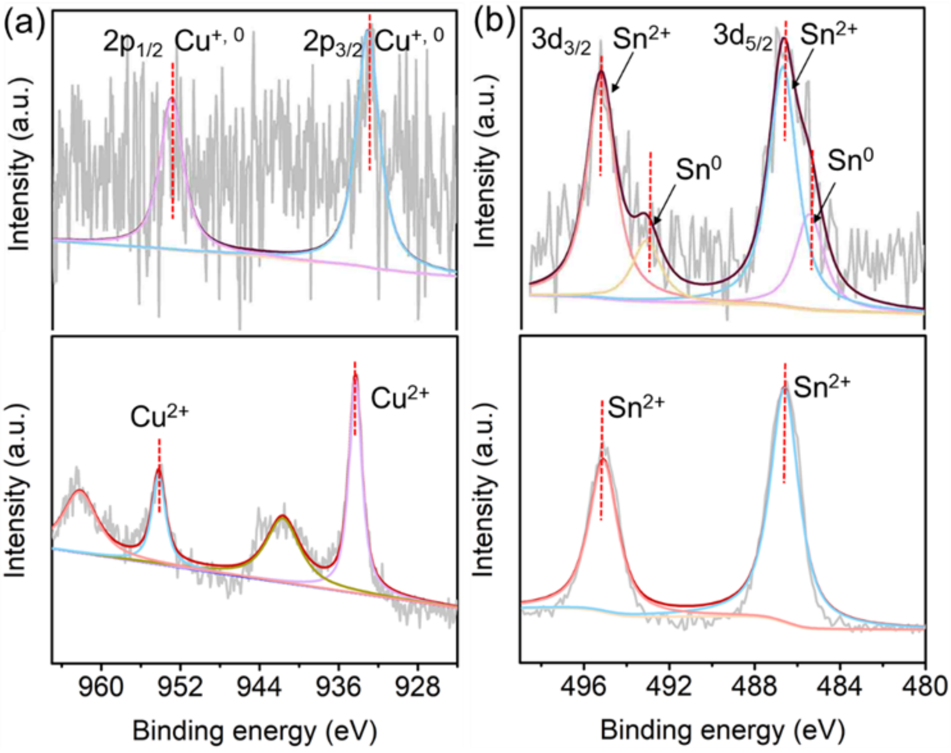

Fig. S9 (a) Cu 2p and (b) Sn 3d for Cu_9Sn_1 alloy catalyst (the upper) and CuSnBDC (9:1) (the lower).

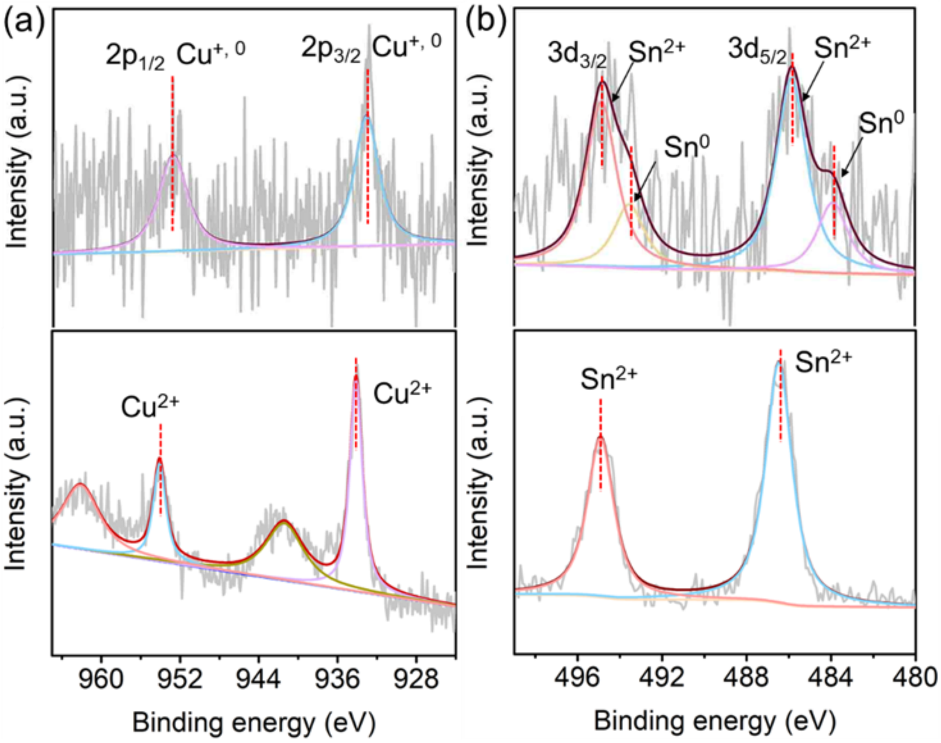

Fig. S10 (a) Cu 2p and (b) Sn 3d for $Cu_{19}Sn_1$ alloy catalyst (the upper) and CuSnBDC (the lower).

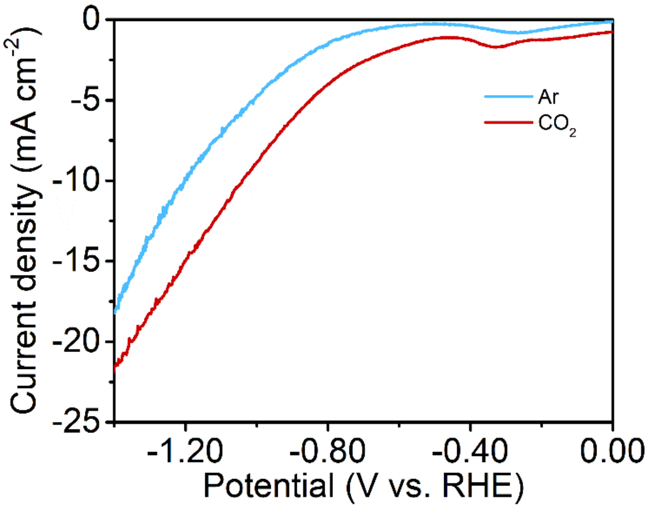

Fig. S11 Linear voltammetry curve of Cu_2Sn_1 alloy catalyst.

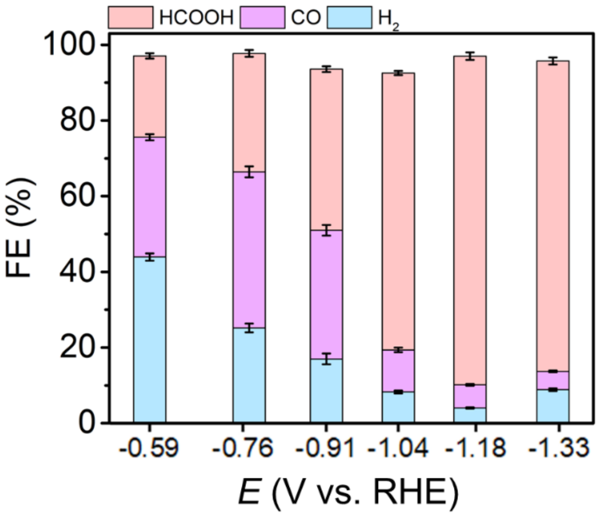

Fig. S12 FE values at different potentials of Cn_1Sn_1 alloy catalyst.

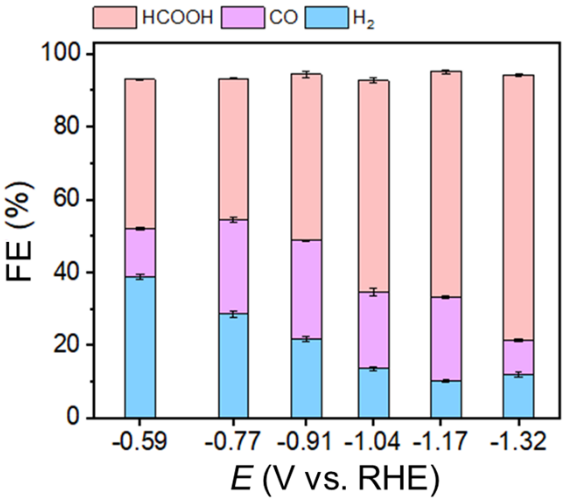

Fig. S13 FE values at different potentials of Cn_4Sn_1 alloy catalyst.

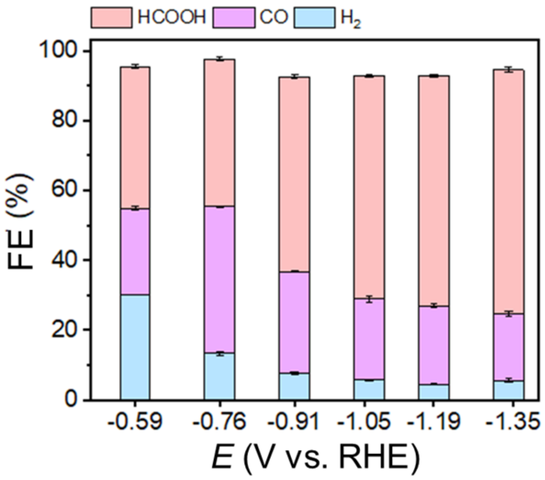

Fig. S14 FE values at different potentials of Cn_9Sn_1 alloy catalyst.

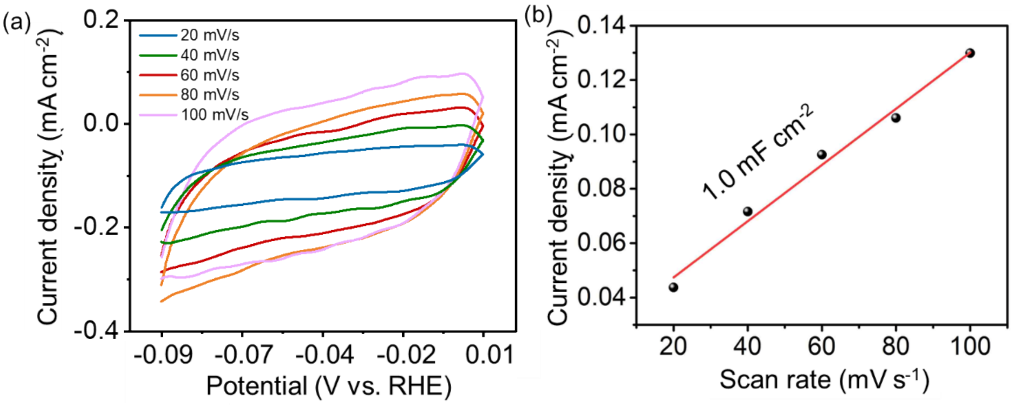

Fig. S15 Cyclic voltammogram curves performed at various scan rates (20, 40, 60, 80, and 100 mV s^{-1}) on the Cu_2Sn_1 alloy catalyst.

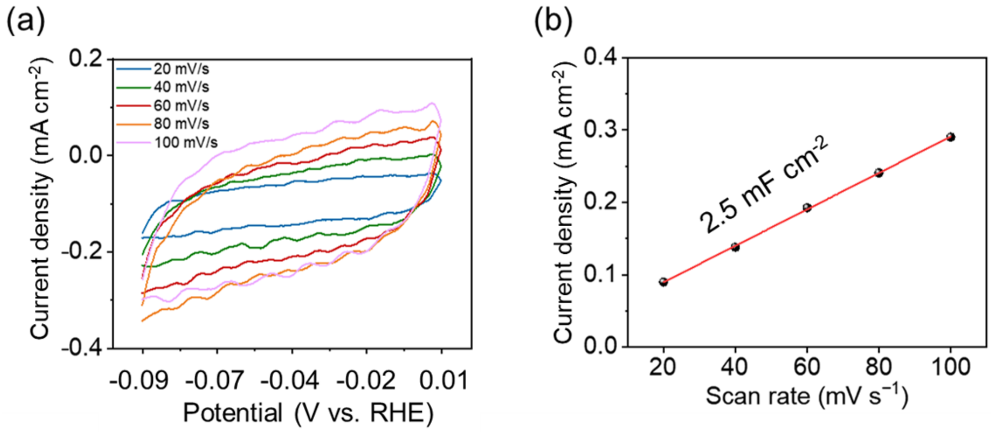

Fig. S16 Cyclic voltammogram curves performed at various scan rates (20, 40, 60, 80, and 100 mV s^{-1}) on the Cu_9Sn_1 alloy catalyst.

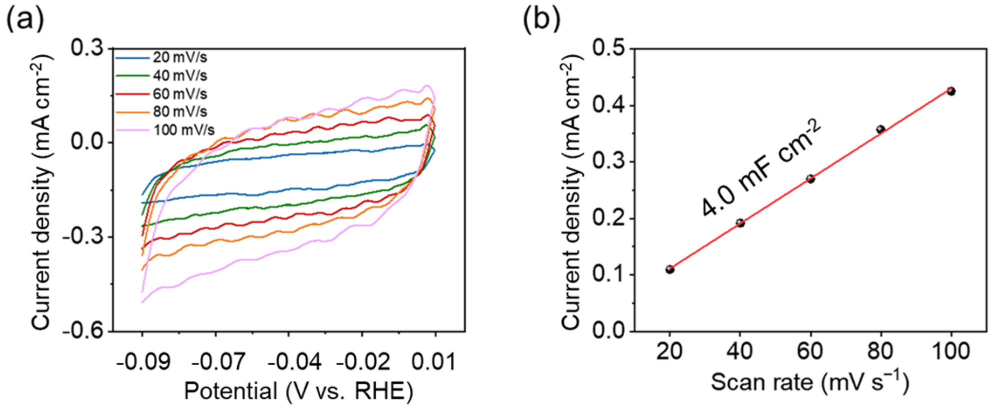

Fig. S17 Cyclic voltammogram curves performed at various scan rates (20, 40, 60, 80, and 100 mV s^{-1}) on the $Cu_{19}Sn_1$ alloy catalyst.

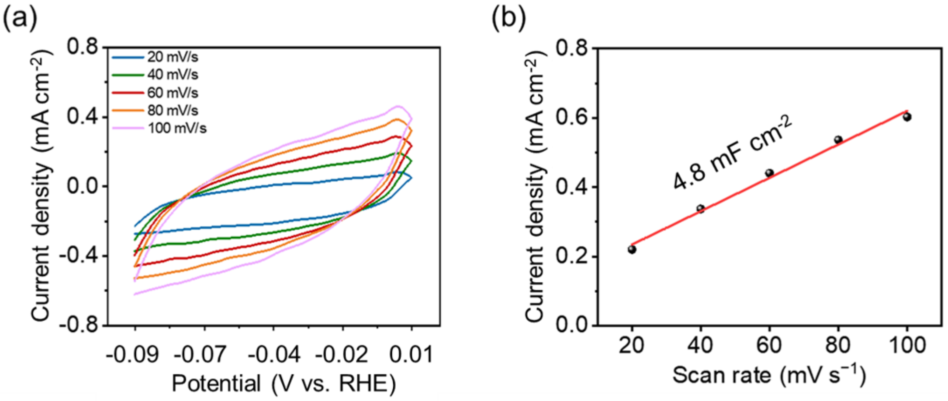

Fig. S18 Cyclic voltammogram curves performed at various scan rates (20, 40, 60, 80, and 100 mV s^{-1}) on the Cu catalyst.

Capacitive currents are plotted against scan rates at −0.65 V vs. RHE to obtain the double-layer capacities (C_{dl}, mF cm^{-2}) based on the slopes of these plots.

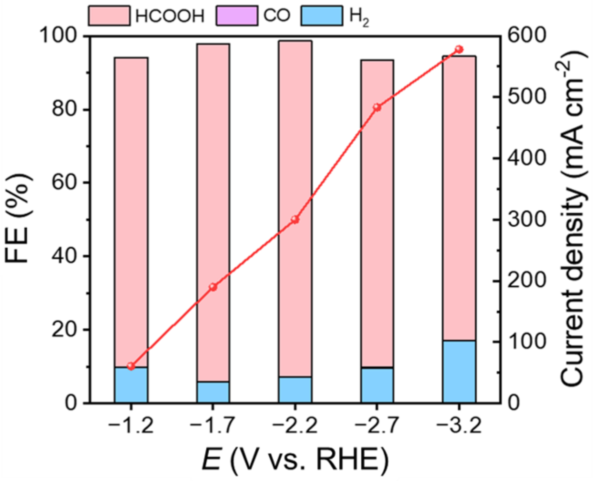

Fig. S19 FE and current density values at different potentials of Cn_2Sn_1 alloy catalyst in the flow cell.

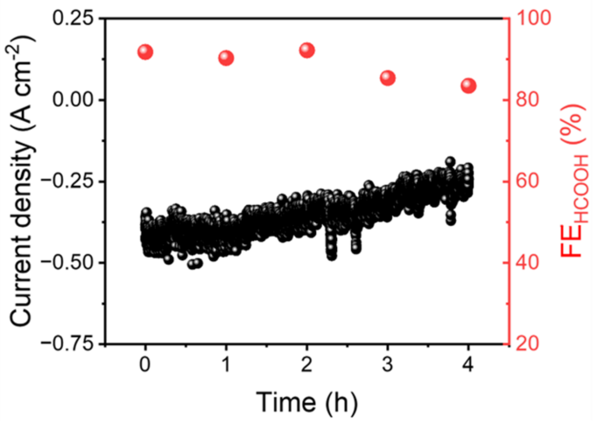

Fig. S20 Stability test of Cu_2Sn_1 alloy catalyst.

Table S1 The Cu: Sn ratios of the investigated CuSn alloy catalysts measured by ICP.

Sample	Input ratio Cu: Sn	CuSnBDC Cu: Sn	CuSn alloy Cu: Sn
Cu	——	——	——
Cu_1Sn_1	1	1.20	1.06
Cu_2Sn_1	2	2.23	2.18
Cu_4Sn_1	4	4.15	4.14
Cu_9Sn_1	9	9.23	9.31
$Cu_{19}Sn_1$	19	18.98	19.02